대한영상의학회지

Value of Image Subtraction for the Identification of Hepatocellular Carcinoma Capsule on Gadoxetic Acid-Enhanced MRI
가도세틱산–조영증강 MRI에서 간세포암 피막 발견에 대한 영상차감기법의 진단적 가치

Hyunjung Kim, MD[1], Jhii-Hyun Ahn, MD[1]*, Jin Sil Moon, MD[2], Seung-Whan Cha, MD[1]

Department of [1]Radiology, [2]Center of Biomedical Data Science, Yonsei University Wonju College of Medicine, Wonju Severance Christian Hospital, Wonju, Korea

Purpose: To evaluate value of image subtraction for identifying hepatocellular carcinoma (HCC) capsule on gadoxetic acid-enhanced MR images.

Materials and Methods: This study involved 108 patients at risk of HCC preoperatively examined using gadoxetic acid-enhanced MRI with hepatic resection between May 2015 and February 2017. We evaluated qualities of subtraction images and presence of capsular appearance on portal venous or transitional phases conventional and subtraction images. We assessed effect of capsular appearance on subtraction images on HCC.

Results: After excluding 1 patient who had treated by transarterial chemoembolization prior to surgery and 33 patients with unsatisfactory subtraction image qualities, 82 focal hepatic lesions (73 HCC, 5 non-HCC malignancies, and 4 benign) from 74 patients were analyzed. Regarding detection of capsules, sensitivity, accuracy, and area under the receiver operating characteristic curve (AUC) on subtraction images were significantly higher than those on conventional images (95.4%, 89.0%, and 0.80, respectively; $p < 0.001$), though specificities were same (64.7%). For diagnosis of HCC, sensitivity, accuracy, and AUC on subtraction images were significantly higher than on conventional images (82.2%, 79.3%, and 0.69, respectively; $p = 0.011$), though specificities were identical (55.6%).

Conclusion: Portal venous or transitional phase gadoxetic acid-enhanced MRI subtraction images could improve detection of HCC capsule.

INTRODUCTION

Hepatocellular carcinoma (HCC) is the fifth most common cancer globally (1). HCC capsules that develop during hepatocarcinogenesis are characteristic of nodular HCC (2). These capsules consist of peritumoral fibrosis and prominent sinusoids, and are observed in about 70% of nodular HCCs (3, 4). Therefore, the presence and identification of capsules are important for the non-invasive diagnosis of HCC. The United Network for Organ Sharing (UNOS)-Organ procurement transplant network (OPTN) system and the Liver Imaging Reporting and Data System (LI-RADS) include an encapsulated appearance as a feature of HCC (5, 6). Furthermore, the existence of an intact capsule is associated with better survival rates and lower recurrence rates after resection or ablative therapy (7, 8).

Contrast-enhanced MRI using dynamic contrast enhanced T1-weighted gradient echo sequences is the most reliable technique for detecting HCC capsules (4, 9). Extracellular and hepatobiliary gadolinium-based contrast agents (gadoxetic acid; Primovist or Eovist; Bayer Healthcare, Berlin, Germany) are commonly used for liver MRI. However, since the pharmacokinetic and pharmacodynamics of these two contrast agents dif-

fer, they have different effects on capsule appearances. Some investigators have reported capsular appearance of HCC is less frequently observed and less discernable on gadoxetic acid-enhanced MR images due to relatively high backgrounds of hepatic parenchymal enhancement (10-12).

Subtraction of unenhanced images from gadolinium-enhanced images has been reported to enable better characterization of the enhancement patterns of focal liver lesions and to maximize lesion visualization (13-15). In the present study, we evaluated the usefulness of subtraction images generated from portal or transitional phase (TP) images with respect to the detection of HCC capsule on gadoxetic acid-enhanced MR images.

MATERIALS AND METHODS

Patients

Our Institutional Review Board approved this retrospective study and waived the requirement for informed consent due to its retrospective nature (IRB No. CR316128). From May 2015 to February 2017, a total of 108 consecutive patients at risk of HCC (91 with liver cirrhosis and 17 with chronic viral hepatitis) underwent preoperative gadoxetic acid-enhanced liver MRI and hepatic resection within 3 months. One patient who had been treated by transarterial chemoembolization prior to surgery was excluded. The remaining 107 patients (71 men, 36 women; mean age, 64 years; range, 45–88 years) had 122 focal hepatic lesions, that is; 108 HCCs, 6 cholangiocarcinomas, 2 combined HCC and cholangiocarcinoma, 1 metastatic adenocarcinoma, 1 high grade dysplastic nodule, 1 regenerative nodule, 2 focal nodular hyperplasia-like nodules, and one intrahepatic splenosis. Eleven patients had multiple HCCs (9 had two HCCs, one had three HCCs, and one had four HCCs) and one patient had one HCC with one combined HCC and cholangiocarcinoma.

MRI Technique

MRI was performed using a 3.0-Tesla system (Magnetom Skyra; Siemens, Erlangen, Germany) equipped with an abdominal 64-channel surface coil. Localizer images were obtained in the supine position, and spectrally fat-suppressed breath-hold T2-weighted turbo spin echo images [repetition time (TR) = 920 ms, echo time (TE) = 106 ms, flip angle = 120°, echo train

length = 94, slice thickness = 5 mm] were obtained in the axial plane. After obtaining a double-echo chemical shift gradient-echo sequence [TR = 4.46 ms, first-echo TE = 1.42 ms (opposed-phase), second-echo TE = 2.85 ms (in-phase), flip angle = 9°], dynamic studies were performed using a three-dimensional gradient echo sequence (VIBE; Siemens) with ultrafast image reconstruction using parallel imaging algorithms (GRAPPA factor = 2) in the axial plane (TR = 4.2 ms, TE = 2.0 ms, flip angle = 13°, matrix = 352 × 192, field of view = 345 × 380 mm, slice thickness = 2.2 mm, slice spacing = 0 mm, slices = 96) during a 20-second breath-holding period. For dynamic studies, gadoxetic acid disodium (0.1 mL/kg) (Primovist; Bayer Healthcare, Berlin, Germany) was administered at 2 mL/s with a power injector as a rapid bolus immediately followed by a 30 mL saline flush. Images were acquired before and after the intravenous injection of gadoxetic acid disodium. The acquisition delay for the arterial phase was usually 20–30 seconds and was determined using a bolus-tracking technique or a test-bolus injection technique. Dynamic images were obtained 30, 60 (portal venous phase, PVP), 180 (TP) and 300 seconds after injection. Hepatobiliary phase images were obtained 20 minutes after contrast injection. Unenhanced images were electronically subtracted from arterial, portal venous, and TPs by an MRI technologist using the system's commercially available software. All scans were forwarded to a picture archiving and communication system.

Image Analysis

One board-certified abdominal radiologist with 4 years of experience, who was not involved in the subsequent image analysis, prepared a list indicating the size and locations of histopathology-proven lesions to be analyzed without indicating any imaging features.

Two board-certified abdominal radiologists (with 11 and 18 years of experience of liver MRI, respectively) blinded to final diagnoses, independently analyzed the MR images. During the image interpretation, the readers referred to the list indicating the anatomic locations and sizes of target lesions to ensure correct identification. After completing the independent review, two readers resolved discordances by discussion and achieved consensus in all cases. Interobserver agreement was assessed using kappa statistics.

The two readers also analyzed the image qualities of subtraction images using the following 5-point scale (16): 1) denoted overall nondiagnostic image quality, 2) denoted severe subtraction artifacts (maximum thickness of subtraction bands of > 5 mm or more than two–thirds of either liver margins or vascular markings ill-defined), 3) denoted moderate subtraction artifacts (maximum thickness of subtraction bands of 2.5 mm, or between one–third and two–thirds of either the liver margins or vascular markings ill defined), 4) denoted good overall image quality with minimal artifacts (maximum thickness of subtraction bands < 2 mm, or less than one-third of either the liver margins or vascular markings ill-defined), and 5) denoted perfect overall subtraction quality without any artifacts. Grades 4 and 5 were considered to indicate satisfactory image quality for subtraction images. Lesions with unsatisfactory image qualities were excluded from further evaluation.

The readers determined the presence or absence of a capsular appearance (a peripheral rim of smooth hyperenhancement) on PVP and/or TP, and LI-RADS categories: (LR-1; definitely benign, LR-2; probably benign, LR-3; indeterminate, LR-4; probably HCC, LR-5; definitely HCC, LR-5V; tumor in vein, and LR-M; probably malignant, but not specific for HCC) for each of the 82 focal hepatic lesions. Two weeks later (to avoid a recall bias), the readers determined the presence or absence of a capsule on subtraction images of PVP and/or TP, and LI-RADS categories of each of the hepatic lesions.

Statistical Analysis

The detection rates of an capsular appearance by visual assessment of PVP and/or TP and using subtraction images of PVP and/or TP were compared using receiver operating characteristic (ROC) curve analysis.

To assess the clinical effects of subtraction images for the diagnosis of HCC using the LI-RADS diagnostic algorithm, we compared the sensitivities, specificities, and accuracies of LR-5 or LR-5V for HCC between the following two situations: 1) when conventionally defined capsular appearance was included as a major feature, and 2) when capsular appearance defined on subtracted images was included as a major feature. Pathological results were used as reference standards.

Interobserver agreement between imaging findings (before consensus) was determined using weighted kappa statistics.

Levels of agreement were defined as follows: poor, $\kappa \leq 0.20$; fair, $\kappa = 0.21–0.40$; moderate, $\kappa = 0.41–0.60$; good, $\kappa = 0.61–0.80$; excellent, $\kappa = 0.81–1.00$. Two-sided p values of less than 0.05 were considered to indicate statistical significance. The analysis was performed using SAS 9.4 (SAS Institute Inc., Cary, NC, USA), MedCalc software (MedCalc Software, Ostend, Belgium), and R 3.1.0 (R Foundation for Statistical Computing, Vienna, Austria).

RESULTS

Image Quality of Subtraction Images

Thirty-three of the 107 patients (30.8%) showed a misregistration artifact (Grade 1, one patient; Grade 2, five patients; and Grade 3, 27 patients), and the images concerned were considered unsatisfactory.

Patient and Lesion Characteristics

After excluding the 33 patients with unsatisfactory subtraction images, we finally analyzed 74 patients with 82 focal hepatic lesions (73 HCCs, 2 cholangiocarcinomas, 2 combined HCC and cholangiocarcinoma, 1 metastatic adenocarcinoma, 1 high grade dysplastic nodule, 1 regenerative nodule, and 2 focal nodular hyperplasia-like nodules). The baseline characteristics of the 74 patients and 82 focal hepatic lesions are summarized in Table 1.

Pathologically, 63 (86.3%) of the 73 HCCs and 2 (40%) of the 5 other malignancies (1 combined HCC and cholangiocarcinoma, 1 cholangiocarcinoma) had a fibrous capsule. None of 4 benign lesions had a capsule.

Image Analysis

Imaging evaluations of capsules revealed good agreement between the two reviewers on conventional ($\kappa = 0.68$) and subtraction images ($\kappa = 0.72$). Diagnostic performances of hepatocellular capsules on conventional images and subtraction images are summarized in Table 2. The sensitivity and accuracy of detection of HCC on subtraction images were higher than those on conventional images, but specificity did not differ. In addition, area under ROC curve (AUC) was significantly higher for subtraction images than conventional images ($p < 0.001$) (Fig. 1).

When focal hepatic lesions were categorized using subtrac-

tion images, the AUC of LR-5 or LR-5V for diagnosing HCC were significantly higher than the AUC of conventional images (0.65 and 0.69, respectively) ($p = 0.011$) (Table 3).

DISCUSSION

In the present study, it was found subtraction images detected the capsular appearance of HCC more sensitively than conven-

tional images (95.4% and 73.9%, respectively) without loss of specificity (64.7% and 64.7%, respectively), and that the diagnostic performances of LR-5 and LR-5V, including capsular appearance as a major feature, using subtraction images was significantly higher than that of conventional images ($p = 0.011$).

Histologically, HCC capsules are composed of two layers; an inner layer rich in fibrous tissue and an outer, water-rich layer with portal venules (or sinusoids) and newly-formed bile ducts (3, 4). However, imaging does not always show a true fibrous capsule; instead, a pseudocapsule consisting of peritumoral sinusoids and/or fibrosis may be evident (4, 17). This capsular appearance, be it a true fibrous capsule or pseudocapsule, is one of the specific findings of HCC, because benign nodules and non-HCC malignancies usually do not manifest a capsular appearance (18-22).

Fibrous capsules and pseudocapsules have similar appearances on dynamic MR images, and appear as enhancing rims on PVP or TP images due to retention of contrast agent within prominent peritumoral sinusoids and/or fibrosis (9). Approximately 50% of gadoxetic acid is uptaken by hepatocytes, and this uptake starts with first pass through the liver; in fact, it has been reported to become visible as early as 90 sec after injection (23). Furthermore, this rapid uptake by hepatocytes also explains the rapid removal of gadoxetic acid from capsule sinusoids, and therefore, capsules are faint and not well identified on PVP or TP images.

However, according to our results, the conspicuity of a capsule or pseudocapsule is improved on subtraction images generated from PVP or TP images. One possible explanation for this result might be that subtraction images more prominently represent subtle differences in contrast enhancement than conventional images, which in turn suggests subtraction images better depict capsular appearance than conventional images.

Table 1. Clinical Characteristics of 74 Patients at Risk of HCC

Characteristic	Value
Patient	
Total	74 (100)
Age (years)	62 [45–86]
Sex	
Male	56 (75.7)
Female	18 (24.3)
Risk factor for HCC	
Hepatitis B viral liver cirrhosis	36 (48.6)
Hepatitis C viral liver cirrhosis	6 (8.1)
Alcoholic liver cirrhosis	13 (17.6)
Chronic hepatitis B	11 (14.9)
Chronic hepatitis C	2 (2.7)
Other*	6 (8.1)
Tumor	
Total	82
Pathologic diagnosis	
HCC	73 (89)
Other malignancies	5 (6.1)
Benign	4 (4.9)
Tumor size (cm)	
HCC	2.8 [0.8–11.8]
Other malignancies	4.7 [1.5–10.5]
Benign	2.1 [0.7–4.3]

Data are n (%) or median [range] values of patients or focal hepatic lesions.
*IIncludes cirrhosis with nonalcoholic steatohepatitis ($n = 3$) or cryptogenic cirrhosis ($n = 3$).
HCC = hepatocellular carcinoma

Table 2. Comparison of the Diagnostic Performances of Conventional and Subtraction Images for the Detection of HCC on Gadoxetic Acid–Enhanced MR Images

	TP	FN	FP	TN	Sensitivity* (95% CI)	Specificity* (95% CI)	Accuracy* (95% CI)	AUC (95% CI)
Conventional image	48	17	6	11	73.9 (61.5–84.0)	64.7 (38.3–85.8)	72.0 (60.9–81.3)	0.69 (0.58–0.79)
Subtraction image	62	3	6	11	95.4 (87.1–99.0)	64.7 (38.3–85.8)	89.0 (80.2–94.9)	0.80 (0.70–0.88)
p value (conventional vs. subtraction)								< 0.001

*Data are % (95% CI) values.
AUC = area under the receiver operating characteristic curve, CI = confidence interval, FN = false negative, FP = false positive, HCC = hepatocellular carcinoma, TN = true negative, TP = true positive
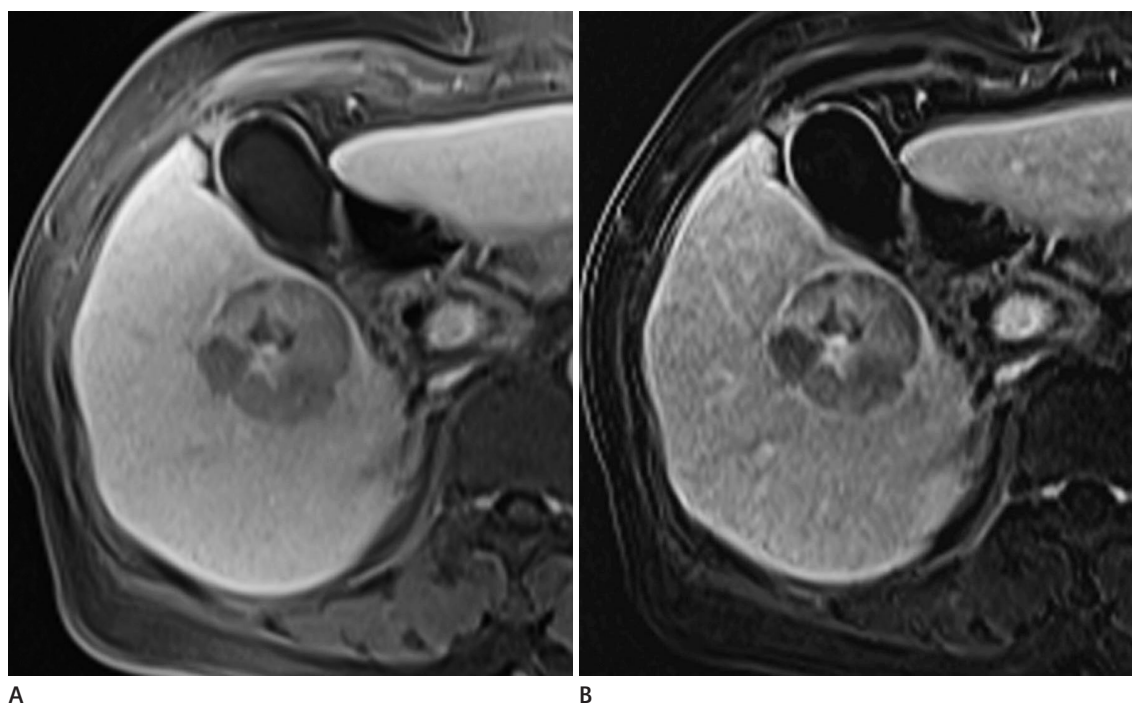
Fig. 1. Case of a 73-year-old woman with hepatocellular carcinoma encased by a histopathologically confirmed fibrous capsule in the right liver.
A. A conventional capsular appearance is not well visualized in the conventional TP image.
B. However, a smooth hyperintense rim is readily detected on the subtracted TP image.
TP = transitional phase

Table 3. Comparison of the Diagnostic Performances of LR–5 or LR–5V for HCC

	TP	FN	FP	TN	Sensitivity* (95% CI)	Specificity* (95% CI)	Accuracy* (95% CI)	AUC (95% CI)
Conventional image	54	19	4	5	74.0 (62.4-83.5)	55.6 (21.2-86.3)	72.0 (60.9-81.3)	0.65 (0.53-0.75)
Subtraction image	60	13	4	5	82.2 (71.5-90.2)	55.6 (21.2-86.3)	79.3 (68.9-87.4)	0.69 (0.58-0.79)
p value (conventional vs. subtraction)								0.011

*Data are % (95% CI) values.
AUC = area under the receiver operating characteristic curve, CI = confidence interval, FN = false negative, FP = false positive, HCC = hepatocellular carcinoma, TN = true negative, TP = true positive

Although some investigators have found that the capsular appearance does not increase diagnostic accuracy for HCC (20), others have asserted that a visualization of a capsule is valuable, as it permits diagnosis of HCC without a definite washout appearance (6, 24). Furthermore, capsular appearance is included as a major imaging feature in the LI-RADS diagnostic algorithm and plays an important role in the diagnosis of HCC. This algorithm considers a hyperintense capsular appearance during PVP or TP as a major diagnostic feature of non-invasive HCC (6), and diagnostic performances of LR-5 and LR-5V using capsular appearance on subtraction images for HCC, are higher than that of conventional imaging. Our results imply that subtraction images can perform an important compensatory role in terms of evaluating capsular appearance when hepatobiliary contrast agents are used. According to recent literature, in patients at risk of developing HCC, a combination of arterial phase hyperenhancement plus washout or a capsular appearance has near 100% specificity for HCC (10). However, in the present study, the specificities of LR-5 and LR-5V for HCC were poor (55.6%), which appeared to be related to several false positive results attributed to the presence of a pseudocapsule.

Previous studies have reported the success of the subtraction technique depends on the degree of misregistration artifact between non-enhanced and enhanced source images (13, 14). The assessment of subtraction image quality is important because false positive diagnoses can be made for capsules when

misregistration occurs. In our study, subtraction image quality was unsatisfactory for 33 of the 107 patients (30.8%) showed (Grade 1 in one patient; Grade 2 in five patients; and Grade 3 in 27 patients). Although image quality was unsatisfactory in many patients, the accuracy of capsule detection was high when subtraction images were of Grade 4 quality or better. There were 6 false positive cases for capsular appearance on subtraction images, and all of these cases produced a false positive result on conventional images. Therefore, these 6 false positive cases were considered to be due to pseudocapsules rather than to misregistration of subtraction images. Nevertheless, unavoidable slice misregistration is the main pitfall of subtraction techniques. Reliable error-correction processing methods for subtraction imaging are needed (14).

This study has several limitations that warrant consideration. First, the sample size was too small to permit definitive conclusions, although all lesions including were confirmed histopathologically. The study was powered to detect a > 10% difference in capsule detection rates with an α of 0.05. Based on the actual sample size, the study has a statistical power of 76.0%. Further studies on larger populations are needed to confirm the value of subtraction images for HCC capsule detection. Second, the retrospective nature of the present study inherently introduces the possibility of patient selection bias. Finally, a 2-week interval may have been insufficient to avoid recall bias.

In summary, we conclude subtraction images from portal or TP images may be helpful for detecting HCC tumor capsules on gadoxetic acid-enhanced MR images in at-risk patients.

REFERENCES

1. El-Serag HB, Davila JA, Petersen NJ, McGlynn KA. The continuing increase in the incidence of hepatocellular carcinoma in the United States: an update. *Ann Intern Med* 2003; 139:817-823.

2. Kojiro M. Histopathology of liver cancers. *Best Pract Res Clin Gastroenterol* 2005;19:39-62

3. Kadoya M, Matsui O, Takashima T, Nonomura A. Hepatocellular carcinoma: correlation of MR imaging and histopathologic findings. *Radiology* 1992;183:819-825

4. Ishigami K, Yoshimitsu K, Nishihara Y, Irie H, Asayama Y, Tajima T, et al. Hepatocellular carcinoma with a pseudocapsule on gadolinium-enhanced MR images: correlation with histopathologic findings. *Radiology* 2009;250:435-443

5. Organ Procurement and Transplantation Network. OPTN/UNOS policy 9.3.G.iv. Available at: http://optn.transplant.hrsa.gov/ContentDocuments/OPTN_Policies.pdf-nameddest=Policy_09. Published Jan 1, 2015. Accessed Mar 16, 2016

6. Liver Reporting and Data System, version 2013.1. American College of Radiology Available at: http://www.acr.org/Quality-Safety/Resources/LIRADS/. Accessed Mar 16, 2016

7. Miraglia R, Pietrosi G, Maruzzelli L, Petridis I, Caruso S, Marrone G, et al. Predictive factors of tumor response to trans-catheter treatment in cirrhotic patients with hepatocellular carcinoma: a multivariate analysis of pre-treatment findings. *World J Gastroenterol* 2007;13:6022-6026

8. Ng IO, Lai EC, Ng MM, Fan ST. Tumor encapsulation in hepatocellular carcinoma. A pathologic study of 189 cases. *Cancer* 1992;70:45-49

9. Grazioli L, Olivetti L, Fugazzola C, Benetti A, Stanga C, Dettori E, et al. The pseudocapsule in hepatocellular carcinoma: correlation between dynamic MR imaging and pathology. *Eur Radiol* 1999;9:62-67

10. Choi JY, Lee JM, Sirlin CB. CT and MR imaging diagnosis and staging of hepatocellular carcinoma: part II. Extracellular agents, hepatobiliary agents, and ancillary imaging features. *Radiology* 2014;273:30-50

11. Dioguardi Burgio M, Picone D, Cabibbo G, Midiri M, Lagalla R, Brancatelli G. MR-imaging features of hepatocellular carcinoma capsule appearance in cirrhotic liver: comparison of gadoxetic acid and gadobenate dimeglumine. *Abdom Radiol (NY)* 2016;41:1546-1554

12. Hope TA, Fowler KJ, Sirlin CB, Costa EA, Yee J, Yeh BM, et al. Hepatobiliary agents and their role in LI-RADS. *Abdom Imaging* 2015;40:613-625

13. Yu JS, Kim YH, Rofsky NM. Dynamic subtraction magnetic resonance imaging of cirrhotic liver: assessment of high signal intensity lesions on nonenhanced T1-weighted images. *J Comput Assist Tomogr* 2005;29:51-58

14. Yu JS, Rofsky NM. Dynamic subtraction MR imaging of the liver: advantages and pitfalls. *AJR Am J Roentgenol* 2003;180:1351-1357

15. Seçil M, Obuz F, Altay C, Gencel O, Iğci E, Sağol O, et al.

The role of dynamic subtraction MRI in detection of hepatocellular carcinoma. *Diagn Interv Radiol* 2008;14:200-204

16. Sundarakumar DK, Wilson GJ, Osman SF, Zaidi SF, Maki JH. Evaluation of image registration in subtracted 3D dynamic contrast-enhanced MRI of treated hepatocellular carcinoma. *AJR Am J Roentgenol* 2015;204:287-296

17. Cho ES, Choi JY. MRI features of hepatocellular carcinoma related to biologic behavior. *Korean J Radiol* 2015;16:449-464

18. Asayama Y, Nishie A, Ishigami K, Ushijima Y, Takayama Y, Fujita N, et al. Distinguishing intrahepatic cholangiocarcinoma from poorly differentiated hepatocellular carcinoma using precontrast and gadoxetic acid-enhanced MRI. *Diagn Interv Radiol* 2015;21:96-104

19. Khan AS, Hussain HK, Johnson TD, Weadock WJ, Pelletier SJ, Marrero JA. Value of delayed hypointensity and delayed enhancing rim in magnetic resonance imaging diagnosis of small hepatocellular carcinoma in the cirrhotic liver. *J Magn Reson Imaging* 2010;32:360-366

20. Park HJ, Jang KM, Kang TW, Song KD, Kim SH, Kim YK, et al. Identification of imaging predictors discriminating different primary liver tumours in patients with chronic liver disease on gadoxetic acid-enhanced MRI: a classification tree analysis. *Eur Radiol* 2016;26:3102-3111

21. Rimola J, Forner A, Tremosini S, Reig M, Vilana R, Bianchi L, et al. Non-invasive diagnosis of hepatocellular carcinoma ≤ 2 cm in cirrhosis. Diagnostic accuracy assessing fat, capsule and signal intensity at dynamic MRI. *J Hepatol* 2012;56:1317-1323

22. Suh YJ, Kim MJ, Choi JY, Park YN, Park MS, Kim KW. Differentiation of hepatic hyperintense lesions seen on gadoxetic acid-enhanced hepatobiliary phase MRI. *AJR Am J Roentgenol* 2011;197:W44-W52

23. Vogl TJ, Kümmel S, Hammerstingl R, Schellenbeck M, Schumacher G, Balzer T, et al. Liver tumors: comparison of MR imaging with Gd-EOB-DTPA and Gd-DTPA. *Radiology* 1996;200:59-67

24. An C, Rhee H, Han K, Choi JY, Park YN, Park MS, et al. Added value of smooth hypointense rim in the hepatobiliary phase of gadoxetic acid-enhanced MRI in identifying tumour capsule and diagnosing hepatocellular carcinoma. *Eur Radiol* 2017;27:2610-2618

가도세틱산-조영증강 MRI에서 간세포암 피막 발견에 대한 영상차감기법의 진단적 가치

김현중[1] · 안지현[1]* · 문진실[2] · 차승환[1]

목적: 가도세틱산-조영증강 MRI에서 간세포암 피막 발견에 대한 영상차감기법의 진단적 가치를 알아보고자 하였다.

대상과 방법: 2015년 5월부터 2017년 2월까지 가도세틱산-조영증강 MRI를 시행 받고 수술을 시행한 hepatocellular carcinoma (이하 HCC) 고위험군 108명을 대상으로 하였다. 차감영상의 질 및 간문맥기와 이행기의 일반영상과 차감영상에서 피막 여부에 대해 평가하였고, 차감영상에서의 피막 여부가 Liver Imaging Reporting and Data System에 따른 간세포암 진단에 미치는 영향을 평가하였다.

결과: 수술 전 경동맥화학색전술을 시행 받았거나 차감영상의 질이 불만족스러운 34명의 환자를 제외한 74명의 환자에서 82개의 간 병변(간세포암 73개, 그 외 악성종양 5개, 양성종양 4개)에 대해 분석하였다. 피막의 발견에 대한 차감영상의 민감도, 정확도, 그리고 곡선하면적은 일반영상과 비교하여 통계적으로 유의하게 높았고(각 95.4%, 89.0%, 0.80; $p < 0.001$), 특이도는 동일하였다(64.7%). HCC의 진단에 대해서도 차감영상이 일반영상과 비교하여 민감도, 정확도, 그리고 곡선하면적이 통계적으로 유의하게 높았으며(각 82.2%, 79.3%, 0.69; $p = 0.011$), 특이도는 동일하였다(55.6%).

결론: 가도세틱산-조영증강 MRI에서 간문맥기 또는 이행기로부터의 차감영상은 간세포암 피막의 발견에 도움이 된다.

연세대학교 원주의과대학 원주세브란스 기독병원 [1]영상의학과, [2]생의학데이터센터